Dalton Transactions

ROYAL SOCIETY OF CHEMISTRY

PAPER

View Article Online
View Journal | View Issue

Check for updates

Cite this: *Dalton Trans.*, 2020, **49**, 9882

With complements of the ligands: an unusual *S*-shaped $[Mn_7]_2$ assembly from tethered calixarenes†

Marco Coletta, [a,b] Sergio Sanz, [a] Euan K. Brechin *[a] and Scott J. Dalgarno *[b]

Received 16th May 2020,
Accepted 26th June 2020

DOI: 10.1039/d0dt01766c

rsc.li/dalton

The reaction between $MnCl_2{\cdot}4H_2O$, 2,2′-bis-*p*-^{t}Bu-calix[4]arene (H_8L1) and 2-(hydroxymethyl)pyridine (hmpH) in a basic dmf/MeOH solution results in the formation of the complex $[Mn^{III}_{10}Mn^{II}_4(L1)_3(hmp)_4(\mu_3\text{-}O)_4(\mu_3\text{-}OH)_2(MeOH)_4(dmf)_6](dmf)_4$ (**6**) upon vapour diffusion of petroleum ether into the mother liquor. The crystals are in the monoclinic space group *C*2/*c*, with the asymmetric unit (ASU) comprising one half of the molecule. The structure describes a large *S*-shaped cluster (~40 Å top to tail) where the unusual *syn* and *anti* conformations of the calixarene ligands results in two binding pockets each containing a $[Mn^{III}_5Mn^{II}_2]$ moiety comprised of two perpendicular, vertex-sharing $[Mn_4]$ butterflies. One butterfly possesses a $[Mn^{III}_4O_4]$ core and the second a $[Mn^{III}_2Mn^{II}_2O_3]$ unit with the Mn^{II} ions in the central body positions. Magnetic susceptibility and magnetisation measurements reveal weak exchange interactions between the metal centres.

Introduction

The coordination chemistry of Mn remains of interest across a breadth of disciplines ranging from biochemistry[1] to molecular magnetism.[2] Indeed, initial success in the latter owes much to the success of the former – the discovery of slow relaxation of the magnetisation in a $[Mn_{12}]$ complex[3] prompted a glut of magnetic measurements on polymetallic compounds of Mn whose structures had been elucidated primarily as metalloenzyme models.[4–7] These early magneto-structural studies paved the way for research on Single-Molecule Magnets (SMMs) that followed over the next thirty years, and continues to this day.[8,9]

One of the great (synthetic) advantages of using Mn in the construction of polymetallic molecules is its coordinative flexibility, aligned to its ability to commonly exist in three stable oxidation states (II, III, IV), even within the same molecule.[10] This has led to the characterisation of a plethora of coordination compounds with a variety of topologies, that often display magnetic ground states even in the presence of antiferromagnetic exchange.[11] However, this flexibility can also be a problem if one wants to rigidly design a particular architecture – absolute structure prediction is usually not forthcoming, especially when employing coordinatively flexible bridging ligands.[12] This is tempered by the fact that common structural motifs, for example $[Mn_3O]^{n+}$ triangles,[13] $[Mn_4O_2]^{n+}$ butterflies,[14] $[Mn_3O_4]^{n+}$ partial cubanes,[15] $[Mn_4O_4]^{n+}$ cubanes,[16] recur time and again, even from multi-component reactions with vastly different ligand types. One way of exploiting this is to employ co-ligands whose coordination modes are well-established and complementary, with the aim of forming new hybrid structures that display the common structural features akin to both ligand types. To this end, we have been combining hmpH (2-(hydroxymethyl)pyridine) with H_4TBC[4] (*p*-^{t}Bu-calix[4]arene).[17] At first, these may seem like odd bedfellows, but an examination of the library of Mn structures deposited in the Cambridge Structural Database (CSD) reveals both have a preponderance to form structures based on $[Mn_4O_2]^{n+}$ butterflies and/or $[Mn_3O_4]^{n+}$ partial cubanes. For example, the homoleptic compounds $[Mn^{III}_2Mn^{II}_2(hmp)_6Br_2(H_2O)_2]Br_2$[18] (**1**) and $[Mn^{III}_2Mn^{II}_2(TBC[4])_2(\mu_3\text{-}OH)_2(dmf)_6]$[19,20] (**2**) both feature the butterfly topology, albeit with the oxidation state distribution reversed (Fig. 1A and B). Note that the tetraphenolato pocket of TBC[4] is perfectly suited to house a Jahn–Teller (JT) distorted Mn^{III} ion. The first compound we isolated using this combination of ligands is of formula $[Mn^{III}_3Mn^{II}_2(OH)_2(TBC[4])_2(hmp)_2(dmf)_6]$ (**3**, Fig. 1C) whose structure describes two fused partial cubanes.[17]

We have expanded this chemistry to include 2,2′-bis-*p*-^{t}Bu-calix[4]arene (H_8L1, Fig. 1D), a ligand comprising two

[a]*EastCHEM School of Chemistry, The University of Edinburgh, David Brewster Road, Edinburgh, Scotland, EH9 3FJ, UK. E-mail: ebrechin@ed.ac.uk*
[b]*Institute of Chemical Sciences, Heriot-Watt University, Riccarton, Edinburgh, Scotland, EH14 4AS, UK. E-mail: S.J.Dalgarno@hw.ac.uk*

†Electronic supplementary information (ESI) available: Bond valence sum calculations to support oxidation state assignment. CCDC 1997361. For ESI and crystallographic data in CIF or other electronic format see DOI: 10.1039/d0dt01766c

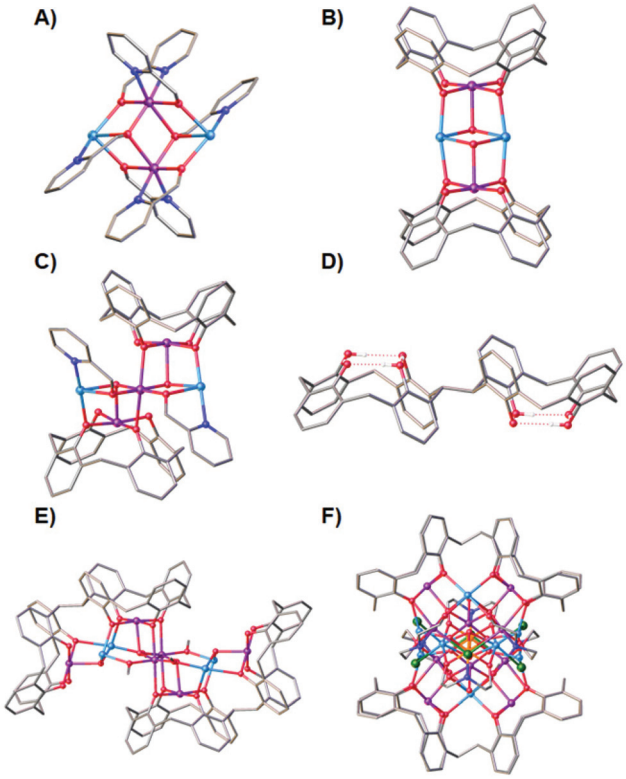

Fig. 1 Single crystal X-ray structures of **1** (A), **2** (B), **3** (C), H_8L1 (D), **4** (E) and **5** (F). Colour code C – grey, O – red, N – royal blue, Mn^{II} – pale blue, Mn^{III} – purple, Cl – green, H – white. Hydrogen atoms (except those involved in lower-rim H-bonding in D), ^{t}Bu groups, ligated solvent molecules and co-crystallised solvent/anions omitted for clarity.

H_4TBC[4]s tethered through one methylene bridge.[21] Indeed, we have recently shown that it is possible to tether H_4TBC[4]s with a range of other linkers of varying degrees of flexibility/rigidity.[22,23] The mobility of H_8L1 gives rise to many conformational possibilities. However, if one of the H_4TBC[4] moieties in Fig. 2 inverts, this changes H_8L1 from an *anti* to *syn* conformation and simultaneously gives rise to new potential binding pockets in the regions between the two constituent tetraphenolic pockets.[24] In line with our exploratory work with H_4TBC[4], we undertook similar studies with H_8L1 with a view to comparing metal-ion binding preferences. In doing so we formed a number of fascinating new polymetallic clusters, all of which closely mirrored the binding preferences of H_4TBC[4] thanks to methylene bridge tethering.[25–28] For example, one can see clear similarities between (**2**) and $[Mn^{III}_6Mn^{II}_4(L1)_2(\mu_3\text{-}O)_2(\mu_3\text{-}OH)_2(\mu\text{-}CH_3O)_4(H_2O)_4(dmf)_8(dmf)_4]$ (**4**, Fig. 1E).[26] We also isolated a heteroleptic eicosanuclear cluster $[Mn^{IV}_2Mn^{III}_{10}Mn^{II}_8(L1)_2(DEA)_6(\mu_4\text{-}O)_4(\mu_3\text{-}O)_6(dmf)_{10}(Cl)_6(H_2O)_2](dmf)_2(MeOH)(H_2O)_3$ (**5**), displaying coordination modes common to both BisTBC[4] and the co-ligand diethanolamine (H_2DEA, Fig. 1F).[29] Herein we present the synthesis, structure and magnetic behaviour of an unusual, and very large, *S*-shaped $[Mn_7]_2$ assembly formed with H_8L1 and hmpH in which L1 is present in both *syn* and *anti* conformations.

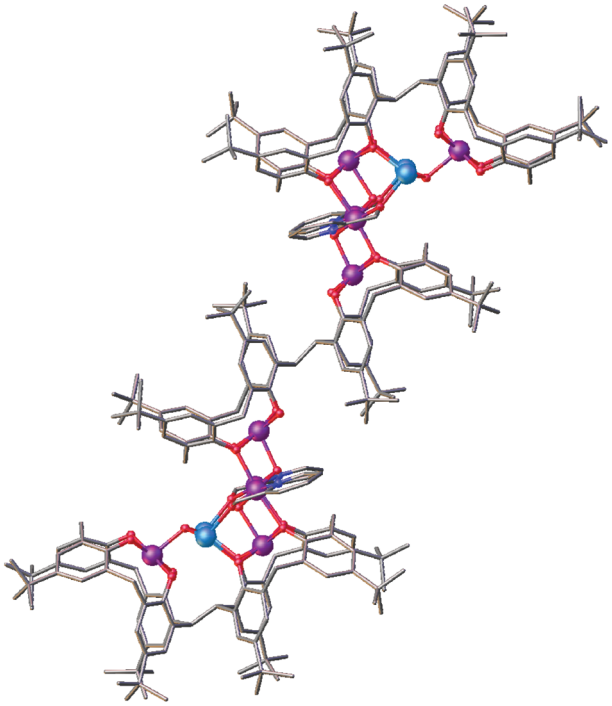

Fig. 2 Symmetry-expanded structure of **6** showing the central bridging *syn*-L octa-anion. Colour code C – grey, O – red, N – royal blue, Mn^{II} – pale blue, Mn^{III} – purple. Hydrogen atoms, ligated solvent molecules and co-crystallised solvent/anions omitted for clarity.

Results and discussion

Reaction of H_8L1 with $MnCl_2{\cdot}4H_2O$ and hmpH in a basic dmf/MeOH solution afforded dark purple single crystals of formula $[Mn^{III}_{10}Mn^{II}_4(L1)_3(hmp)_4(\mu_3\text{-}O)_4(\mu_3\text{-}OH)_2(MeOH)_4(dmf)_6](dmf)_4$ (**6**) upon vapour diffusion of petroleum ether into the mother liquor (Fig. 2). The crystals were found to be in a monoclinic cell and structure solution was performed in the space group *C*2/*c*. The ASU (Fig. 3) comprises one half of the molecule, the $[Mn^{III}_5Mn^{II}_2]$ metallic skeleton of which (Fig. 4) describes two perpendicular, vertex-sharing $[Mn_4]$ butterflies. The two butterflies are rather different, one being homovalent $[Mn^{III}_4O_4]$ (Mn2, Mn3, Mn6, Mn7) and one being a rather unusual $[Mn^{III}_2Mn^{II}_2O_3]$ unit (Mn1, Mn2, Mn4, Mn5) with the Mn^{II} ions in the central body positions. Three of the five Mn^{III} ions (Mn1–3) are located in the TBC[4] cavities, in line with expected ion binding rules,[28] occupying the wing-tip positions of the butterflies. The remaining two Mn^{III} ions (Mn6–7) occupy the body positions of one of the butterflies, being chelated by the μ-hmp ligands, which further bridge to the Mn^{II} ions (Mn4–5) in the body positions of the second butterfly. The latter fill the coordination sites between the two TBC[4] moieties generated through inversion of H_8L1. Mn1 is bound to the four phenolato oxygens of the TBC[4] binding site (O1–O4, with Mn1–O bond distances in the range of 1.891(10)–1.953(10) Å), and has distorted square pyramidal geometry. Its coordination sphere is completed by a μ_3-hydroxide (Mn1–

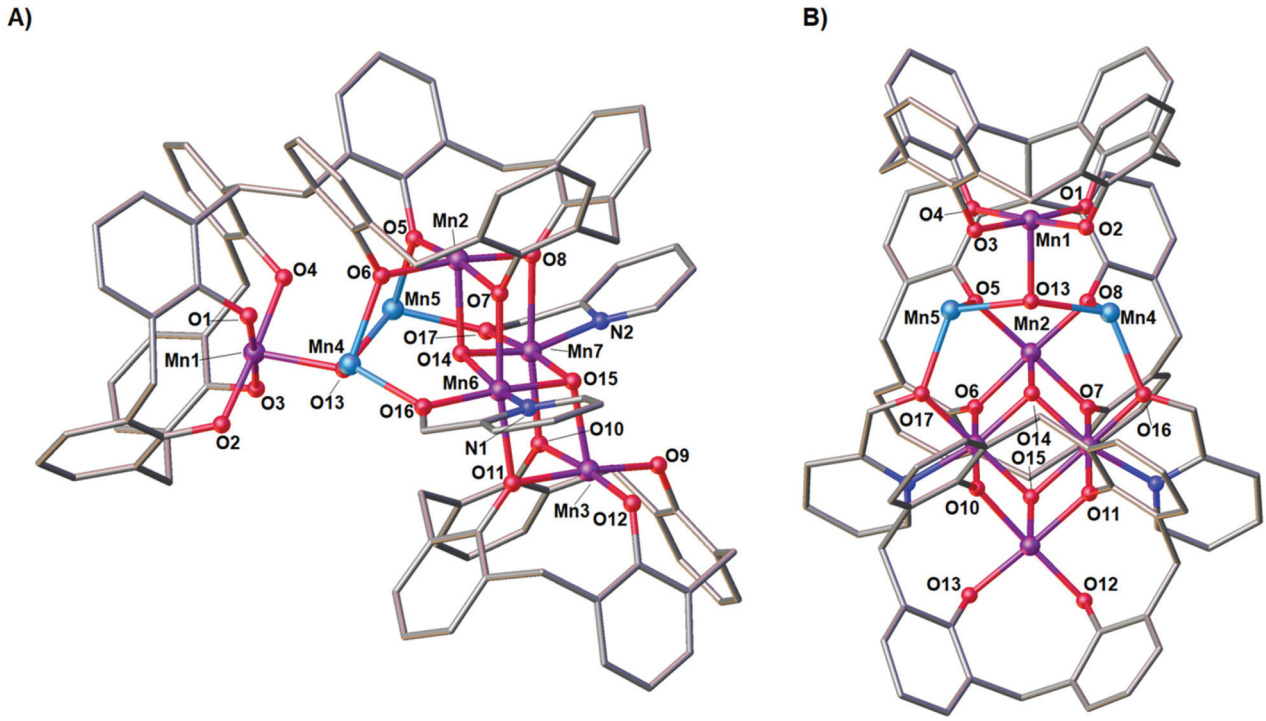

Fig. 3 Side (A) and orthogonal (B) views of the partial single crystal X-ray structure of the asymmetric unit in **6**. Selected labels have been added according to discussion. Colour code C – grey, O – red, N – royal blue, Mn^{II} – pale blue, Mn^{III} – purple. Hydrogen atoms, ^{t}Bu groups, ligated solvent molecules and co-crystallised solvent/anions omitted for clarity. Figures not to scale.

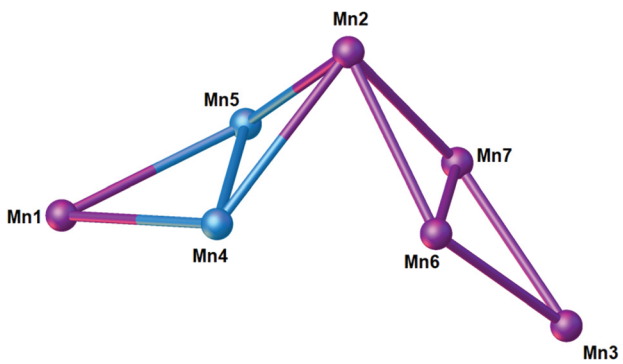

Fig. 4 Metallic skeleton of the $[Mn_7]$ unit in **6** highlighting the two vertex sharing $[Mn_4]$ butterflies. Colour code: Mn^{II} – pale blue, Mn^{III} – purple.

O13, 2.083(9) Å) that bridges to Mn4 and Mn5 (Mn4–O13, 2.191(9) Å and Mn5–O13, 2.187(10) Å). Mn4 and Mn5 are located in the binding site generated by the inversion of L and have distorted trigonal bipyramidal geometry; these have very similar coordination spheres. In addition to the aforementioned μ_3-oxide, they are bonded to a phenolic oxygen (Mn4–O8, 2.116(9) Å and Mn5–O5, 2.128(9) Å), a ligated dmf molecule (Mn4–O19, 2.190(11) Å and Mn5–O20, 2.170(13) Å), a ligated MeOH molecule (Mn4–O21, 2.208(10) Å, Mn5–O22, 2.218(10) Å) and a μ-oxygen of a hmp ligand (Mn4–O16, 2.155(11) Å and Mn5–O17, 2.161(11) Å). Mn2 also occupies a tetraphenolato binding site (O5–O8, with Mn2–O bond distances in the range of 1.917(9)–1.946(9) Å) with a distorted octahedral geometry. Mn2 is bound to a ligated dmf molecule located in a TBC[4] cavity (within the inverted L1, Mn2–O18, 2.206(11) Å) and a μ_3-oxide (Mn2–O14, 2.204(9) Å), the latter bridging to Mn6 and Mn7 (Mn6–O14, 1.896(9) Å and Mn7–O14, 1.865(8) Å). The O14–Mn2–O18 vector defines the Jahn–Teller axis and deviation from linearity is observed at 174.9(4)°. Mn6 and Mn7 have distorted octahedral geometries; the O7–Mn6–O11 and O6–Mn7–O10 bonds define the Jahn–Teller axes, both of which show deviation from linearity at 172.3(3)° and 173.5(4)°, respectively. Both Mn6 and Mn7 are bound to two phenolato oxygen atoms belonging to two TBC[4] moieties from neighbouring L1s (Mn6–O7, 2.284(9) Å; Mn6–O11, 2.189(10) Å; Mn7–O6, 2.292(9) Å and Mn7–O10. 2.171(9) Å), the aforementioned μ_3-oxides (O14 and O15) and a ligated hmp (Mn6–N1, 2.005(13) Å; Mn6–O16, 1.934(10) Å; Mn7–N2, 2.027(13) Å and Mn7–O17, 1.908(11) Å). Finally, Mn3 is coordinated to the lower-rim phenolato oxygens of the half-L in the ASU (O9–O12, with Mn3–O distances in the range 1.916(9)–1.981(9) Å), and has distorted square pyramidal geometry. The Mn3 coordination sphere is completed by a μ_3-oxide (Mn3–O15, 2.119(9) Å) that bridges to Mn6 and Mn7 (Mn6–O15, 1.906(9) Å and Mn7–O15, 1.913(9) Å).

Symmetry expansion reveals the complexity of this large assembly, which can be visualised as two $[Mn^{III}_5Mn^{II}_2]$ clusters bridged by a central octa-anionic L1 (Fig. 2). The assembly measures ~40 Å from top to tail, and this double cluster is par-

ticularly interesting because it breaches the assembly rules we have established to date in a range of experiments with H_8L1. The most noticeable feature in the structure of **6** is that octa-anionic L is present in both a *syn* and *anti*-conformation, meaning that not all L1s have undergone inversion upon metal ion complexation.[24] This is contrary to all previously reported clusters formed with this ligand, and inspection of Fig. 2 and 3 provides the likely reason for this marked variation in behaviour. Incorporation of the hmp co-ligands around the Mn6 and Mn7 centres means that they occupy significant space above O9 and O12 (Fig. 3). The two hmp ligands are also located relatively close to the aromatic rings of one TBC[4] moiety (~4.5 Å), complementarity that we have found to be influential when combining H_4TBC[4] with a range of salicylaldoximes (of varying steric bulk) as co-ligands in Mn-cluster formation. The incorporation of hmp in this new cluster may therefore prevent the central L1 from undergoing conformational inversion and halt extended cluster formation at this point.

By understanding the degree of complementarity between the two ligands, it may be possible to exercise a level of control over the cluster composition and topology through future co-ligand design. Inspection of the extended structure in **6** shows that the molecules form a bi-layer array along the *c* axis as shown in Fig. 5. Hydrogen bonds are found between ligated (Mn5) and co-crystallised dmf molecules with a symmetry unique CH···O distance of 2.525 Å; the shortest metal–metal intercluster distance found is 12.410 Å. This confirms that the clusters are well isolated in the solid state due to the shape and packing behaviour of the constituent TBC[4] moieties. A survey of the CSD for $[Mn^{III}_{10}Mn^{II}_4]$ ($[Mn^{III}_5Mn^{II}_2]$) species, returned a total of 23 (99) hits. Of these none have the same topology or oxidation state distribution. The closest $[Mn_7]$ structure type to the ASU is found in the molecule $(NEt_4)[Mn^{III}_7(OAc)_{10}(dbm)_4]$ whose structure describes two homovalent butterflies fused together through a common Mn^{III} vertex.[30] The combination of H_8L1 and hmp has therefore given rise to a new topology.

Magnetic behaviour

DC (direct current) molar magnetic susceptibility (χ_M) data were measured on a powdered polycrystalline sample of **6** in an applied field B = 0.1 T over the temperature range T = 300–5 K. The experimental data are shown in Fig. 6 in the form of the χ_MT product *versus* T. The room temperature χ_MT value of 47.5 cm^3 K mol^{-1} is as expected for the sum of the Curie constants for ten non-interacting Mn^{III} (s = 2) and four non-interacting Mn^{II} (s = 5/2) ions, assuming g = 2.00. As temperature decreases, the χ_MT product remains constant until ~150 K before decreasing steadily to reach a value of ~36 cm^3 K mol^{-1} at T = 5 K. This behaviour is indicative of the presence of very weak exchange interactions between the constituent metal ions. A fit of inverse susceptibility data to the Curie–Weiss law affords θ = −2.92 K and C = 48.5 cm^3 K mol^{-1} (inset, Fig. 6). Magnetisation data measured in the T = 2–7 K range and B = 0.5–7.0 T range are consistent with this picture, M rising slowly with increasing B without reaching saturation. The presence of very weak exchange is consistent with that

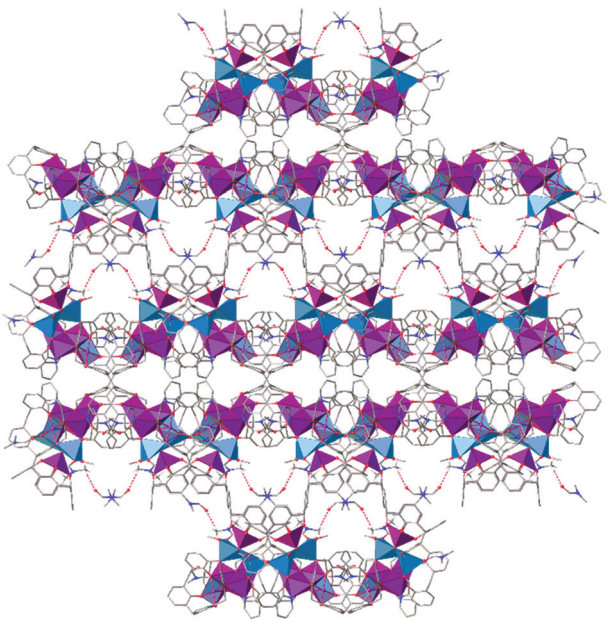

Fig. 5 View of the *ab* plane in the extended structure of **6** showing hydrogen bonding interactions (dashed red lines) between ligated and co-crystallised dmf and the overall bi-layer type array. Colour code C – grey, O – red, N – royal blue, Mn^{II} – pale blue polyhedra, Mn^{III} – purple polyhedra. Hydrogen atoms not involved in H-bonding, ^{t}Bu groups, ligated solvent molecules and co-crystallised solvent/anions omitted for clarity.

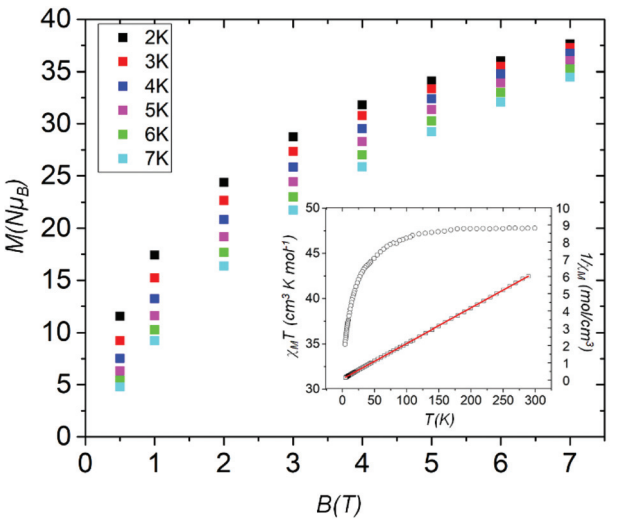

Fig. 6 Field dependence of the magnetisation (M) measured in the T = 2–7 K and B = 0.5–7.0 T temperature and field ranges. The inset shows the plot of χ_MT *vs.* T (○) in the range T = 5–300 K and B = 0.1 T, and the $1/\chi_M$ *vs.* T (□) data. The solid line is a fit of the experimental data to the Curie–Weiss law.

observed in previously published [Mn^{III}_4] butterflies and in compound **2** which show exchange interactions in the $0 \leq |J| \leq 10\ cm^{-1}$ range.[19] There are no frequency-dependent signals in out-of-phase (χ''_M) ac susceptibility measurements.

Experimental section

H_8L1 was synthesised according to literature procedure.[21]

Synthesis of $[Mn^{III}_{10}Mn^{II}_4(L1)_3(hmp)_4(\mu_3\text{-}O)_4(\mu_3\text{-}OH)_2(MeOH)_4(dmf)_6](dmf)_4$, 6: H_8L1 (500 mg, 0.39 mmol), $MnCl_2{\cdot}4H_2O$ (610 mg, 3.08 mmol) and 2-(hydroxymethyl)pyridine (0.149 mL, 1.54 mmol) were suspended in a 1 : 1 dmf/MeOH mixture (20 mL) and stirred for 10 minutes. Et_3N (0.6 mL) was added and the resulting purple solution was stirred for additional 2 hours and then filtered. Petroleum ether vapour was slowly diffused into the mother liquor over several days, affording dark purple crystals suitable for X-ray diffraction studies. Elemental Analysis (%) calculated for **6**, $C_{322}H_{418}Mn_{14}N_{14}O_{48}$ (M = 6022.12): C, 64.22%; H, 7%; N, 3.26%. Found: C, 64.12%; H, 6.72%; N, 3.11%. **Yield** 431 mg (19%). **Crystal data for 6 (CCDC 1997361†):** $C_{322}H_{418}Mn_{14}N_{14}O_{48}$, M = 6022.12, 0.1 × 0.05 × 0.05 mm^3, purple needle, monoclinic, space group $C2/c$ (no. 15), a = 59.816(8) Å, b = 18.706(2) Å, c = 30.329(4) Å, β = 104.498(3)°, V = 32 856(7) $Å^3$, Z = 4, Bruker X8 Apex II CCD Diffractometer, MoKα radiation (λ = 0.71073 Å), T = 100(2) K, $2\theta_{max}$ = 37.904°, 33 347 reflections collected, 12 916 unique (R_{int} = 0.1430). Final GooF = 0.927, R_1 = 0.0990, wR_2 = 0.2779.

Conclusions

To conclude, a combinatorial study involving hmpH and H_8L1 as complementary ligands in Mn coordination chemistry has led to the formation of a highly unusual *S*-shaped cluster of formula $[Mn^{III}_{10}Mn^{II}_4(L)_3(hmp)_4(\mu_3\text{-}O)_4(\mu_3\text{-}OH)_2(MeOH)_4(dmf)_6](dmf)_4$ (**6**) that measures ~40 Å from top to tail. The structure of **6** is comprised of two separate $[Mn^{III}_5Mn^{II}_2]$ units which describe perpendicular, vertex-sharing $[Mn^{III}_4O_4]$ and $[Mn^{III}_2Mn^{II}_2O_3]$ butterflies. The presence of two H_4TBC[4] moieties in H_8L1 has promoted an extension in nuclearity when compared to a single H_4TBC[4] moiety, moving from [Mn_5] (**3**) to [Mn_7]. The hmp co-ligand has had a marked effect on the behaviour of H_8L1 as seen by the incorporation of the ligand in both *syn* and *anti* conformations upon complexation. Logical extension to the nature of the *N*,*O*-ligands employed may allow for augmentation of the nuclearity observed around Mn1, Mn4 and Mn5, or in permitting inversion and full incorporation of the central L. Furthermore, variations in steric effects of the *N*,*O*-ligands will also likely prove to be influential in guiding the formation of new nuclearities as this has been previously observed for H_4TBC[4]. Dc magnetic susceptibility and magnetisation measurements reveal very weak exchange interactions between the metal centres, with a fit of the Curie–Weiss law affording θ = −2.92 K and C = 48.5 cm^3 K mol^{-1}.

Conflicts of interest

The authors report no conflict of interest.

Acknowledgements

We thank the EPSRC for financial support under grant reference numbers EP/I03255X/1 and EP/I031421/1. We also thank Heriot-Watt University for financial support for M. C. through the James-Watt Scholarship programme.

Notes and references

1 K. N. Ferreira, T. M. Iverson, K. Maghlaoui, J. Barber and S. Iwata, *Science*, 2004, **303**, 1831–1838.
2 S. Hill, R. S. Edwards, N. Aliaga-Alcade and G. Christou, *Science*, 2003, **302**, 1015–1018.
3 M. A. Novak, R. Sessoli, D. Gatteschi and A. Caneschi, *Nature*, 1993, **365**, 141–143.
4 K. Wieghardt, *Angew. Chem., Int. Ed.*, 1989, **28**, 1153–1172.
5 *Manganese Redox Enzymes*, ed. V. L. Pecoraro, Verlag-Chemie, New York, 1992.
6 V. K. Yachandra, K. Sauer and M. P. Klein, *Chem. Rev.*, 1996, **96**, 2927–2950.
7 J. B. Vincent and G. Christou, *Adv. Inorg. Chem.*, 1989, **33**, 197–257.
8 G. Aromí and E. K. Brechin, *Struct. Bonding*, 2006, **122**, 1–67.
9 C. J. Milios and R. E. P. Winpenny, *Struct. Bonding*, 2015, **164**, 1–109.
10 C. Papatriantafyllopoulou, E. E. Moushi, G. Christou and A. J. Tasiopoulos, *Chem. Soc. Rev.*, 2016, **45**, 1597.
11 R. Inglis, C. J. Milios, L. F. Jones, S. Piligkos and E. K. Brechin, *Chem. Commun.*, 2012, **48**, 181–190.
12 A. J. Tasiopoulos and S. P. Perlepes, *Dalton Trans.*, 2008, 5537–5555.
13 R. D. Cannon and R. P. White, *Progress in Inorganic Chemistry*, John Wiley & Sons, Ltd, 2007, Volume 36, pp. 195–298.
14 E. Libby, E. A. Schmitt, G. Christou, J. K. McCusker, D. N. Hendrickson and K. Folting, *Inorg. Chem.*, 1991, **30**, 3486–3495.
15 M. W. Wemple, H.-L. Tsai, S. Wang, J. P. Claude, W. E. Streib, J. C. Huffman, D. N. Hendrickson and G. Christou, *Inorg. Chem.*, 1996, **35**, 6437–6449.
16 D. N. Hendrickson, E. A. Schmitt, H. Tsai, Q. Li, J. S. Bashkin, J. B. Vincent, G. Christou, E. Libby, S. Wang, P. D. W. Boyd, J. C. Huffman and K. Folting, *J. Am. Chem. Soc.*, 1992, **114**, 2455–2471.
17 S. M. Taylor, R. D. McIntosh, S. Piligkos, S. J. Dalgarno and E. K. Brechin, *Chem. Commun.*, 2012, **48**, 11190–11192.
18 J. Yoo, A. Yamaguchi, M. Nakano, J. Krzystek, W. E. Streib, L. C. Brunel, H. Ishimoto, G. Christou and D. N. Hendrickson, *Inorg. Chem.*, 2001, **40**, 4604–4616.

19 G. Karotsis, S. J. Teat, W. Wernsdorfer, S. Piligkos, S. J. Dalgarno and E. K. Brechin, *Angew. Chem., Int. Ed.*, 2009, **48**, 8285–8288.
20 S. M. Taylor, G. Karotsis, R. D. McIntosh, S. Kennedy, S. J. Teat, C. M. Beavers, W. Wernsdorfer, S. Piligkos, S. J. Dalgarno and E. K. Brechin, *Chem. – Eur. J.*, 2011, **17**, 7521–7530.
21 L. T. Carroll, P. A. Hill, C. Q. Ngo, K. P. Klatt and J. L. Fantini, *Tetrahedron*, 2013, **69**, 5002–5007.
22 M. Coletta, R. McLellan, J. M. Cols, K. J. Gagnon, S. J. Teat, E. K. Brechin and S. J. Dalgarno, *Supramol. Chem.*, 2016, **28**, 557–566.
23 M. Coletta, R. McLellan, P. Murphy, B. T. Leube, S. Sanz, R. Clowes, K. J. Gagnon, S. J. Teat, A. I. Cooper, M. J. Paterson, E. K. Brechin and S. J. Dalgarno, *Chem. – Eur. J.*, 2016, **22**, 8791–8795.
24 P. Murphy, S. J. Dalgarno and M. J. Paterson, *J. Phys. Chem. A*, 2014, **118**, 7986–8001.
25 R. McLellan, M. A. Palacios, C. M. Beavers, S. J. Teat, S. Piligkos, E. K. Brechin and S. J. Dalgarno, *Chem. – Eur. J.*, 2015, **21**, 2804–2812.
26 M. Coletta, R. McLellan, A. Waddington, S. Sanz, K. J. Gagnon, S. J. Teat, E. K. Brechin and S. J. Dalgarno, *Chem. Commun.*, 2016, **52**, 14246–14249.
27 M. Coletta, R. McLellan, S. Sanz, K. J. Gagnon, S. J. Teat, E. K. Brechin and S. J. Dalgarno, *Chem. – Eur. J.*, 2017, **23**, 14073–14079.
28 M. Coletta, E. K. Brechin and S. J. Dalgarno, *Calixarenes and Beyond*, Springer International Publishing, Switzerland, 2016.
29 M. Coletta, S. Sanz, L. J. McCormick, S. J. Teat, E. K. Brechin and S. J. Dalgarno, *Dalton Trans.*, 2017, **46**, 16807–16811.
30 S. Wang, H.-L. Tsai, W. Streib, G. Christou and D. N. Hendrickson, *J. Chem. Soc., Chem. Commun.*, 1992, 677–679.